IRRIGATION AND DRAINAGE
Irrig. and Drain. **65**: 522–529 (2016)
Published online 29 August 2016 in Wiley Online Library (wileyonlinelibrary.com) **DOI**: 10.1002/ird.2061

CHARACTERISTICS OF WATER AND DROPLET SIZE DISTRIBUTION FROM FLUIDIC SPRINKLERS†

JUNPING LIU*, SHOUQI YUAN AND RANSFORD OPOKU DARKO

Research Centre of Fluid Machinery Engineering and Technology, Jiangsu University, Zhenjiang, Jiangsu, China

ABSTRACT

A new prototype of fluidic sprinkler (PXH) is proposed and its working theory is reported. The hydraulic performance of four different types of sprinkler head (PXH, PY, Toro S 800 and RainBird S 3504) was compared at the same operating pressure. Meanwhile, PXHs with nozzle diameters of 4, 6 and 8 mm were tested to establish a mathematical model of water distribution and droplet diameter. The results show that the PXH produces the longest wetted radius, potentially due to its unique working principles. The PXH exhibits optimal water distribution performance because the air in the nozzle destroys the fluid structure of the water jet. The PXH results in the smallest droplet diameter, which transfers less kinetic energy to the soil. The results from the empirical equations of a distribution model from the PXH were plotted against actual values to obtain regressions, with coefficients of determination ranging from 95.1 to 98.8%. The droplet size model was determined by fitting the experimental results obtained using different operating pressures and nozzle diameters. The model was verified using the experimental results of six cases with different droplet diameters. The average relative error between the predicted and measured droplet diameters was 4.6%. Copyright © 2016 John Wiley & Sons, Ltd.

KEY WORDS: fluidic sprinkler; hydraulic performance; water distribution; droplet size

Received 7 September 2015; Revised 21 April 2016; Accepted 22 April 2016

RÉSUMÉ

Un nouveau prototype de gicleur fluidique (PXH) est. proposé et la théorie de son fonctionnement est. rapportée. Les performances hydrauliques de quatre différents types de têtes de gicleurs (PX, PY, Toro S 800 et S RainBird 3504) ont été comparées à la même pression de fonctionnement. Pendant ce temps, des PXHs avec des diamètres de buse de 4, 6 et 8 mm ont été testés pour établir un modèle mathématique de distribution d'eau et de diamètre des gouttelettes. Les résultats montrent que le PXH produit le rayon le plus long rayon mouillé, potentiellement en raison de ses principes de fonctionnement uniques. Le PXH présente une performance optimale de la distribution de l'eau parce que l'air dans la buse détruit la structure fluidique du jet d'eau. Il en résulte des gouttelettes de petit diamètre, qui transfèrent moins d'énergie cinétique au sol. Les résultats des équations empiriques d'un modèle de distribution de PXH ont été tracés en fonction des valeurs réelles pour obtenir des régressions avec des coefficients de détermination allant de 95.1 à 98.8%. Le modèle de la taille des gouttelettes a été déterminé par ajustement aux résultats expérimentaux obtenus en utilisant différentes pressions de fonctionnement diamètres de buse. Le modèle a été vérifié en utilisant les résultats expérimentaux de six cas avec différents diamètres de gouttelettes. L'erreur relative moyenne entre les diamètres des gouttelettes prédites et mesurées était de 4.6%. Copyright © 2016 John Wiley & Sons, Ltd.

MOTS CLÉS: sprinkler fluidique; performance hydraulique; distribution d'eau; taille des gouttelettes

INTRODUCTION

As water supplies become limited, agricultural water use should become more efficient so that current productivity levels can be maintained. Sprinkler irrigation technology has existed for many years. Recently, sprinkler irrigation has become widely used in agricultural production and covers an area of 2.5 million ha in China (Yan, 2010). The sprinkler head is an important component of sprinkler irrigation systems. The performance of the sprinkler head plays a significant role in irrigation quality.

*Correspondence to: Dr Liu Junping, Jiangsu University, No.301 Xuefu Road, Zhenjiang, Jiangsu 212013, China. E-mail: liujunping401@163.com
†Caractéristiques et distributions de l'eau et de la taille des gouttelettes de sprinklers fluidiques.

Sprinkler heads are commonly used in modern irrigation practices worldwide (Branscheid *et al.*, 1986). Consequently, characterizing the relevance of several designs and managing the factors that affect the efficiency and uniformity of sprinklers are important (Li *et al.*, 2003). Some parameters, such as wetted radius, water distribution, uniformity coefficient and droplet size, are usually regarded as important aspects of performance.

Several modelling approaches for sprinkler irrigation have been developed to predict sprinkler irrigation performance. The sprinkler performance model has been the subject of a series of research efforts since the 1990s (Delirhasannia *et al.*, 2010). Fukui *et al.* (1980) presented basic equations and procedures for the ballistic simulation of sprinkler irrigation. The Christiansen coefficient of uniformity and the water application pattern have been predicted using a ballistic simulation model (Vories *et al.*, 1987; Seginer *et al.*, 1991; Burt *et al.*, 1997; Carrion *et al.*, 2001; Montero *et al.*, 2001; Dechmi *et al.*, 2004a, 2004b; Playan *et al.*, 2006). Smith *et al.* (2008) developed a computer model (TRAVGUN) to simulate irrigation applications using travelling gun machines under different wind conditions. The sprinkler pattern model has been selected as the basis of the decision support system TRAVGUN, which was created by Richards and Weatherhead (1993) and modified by Al-Naeem (1993). A third-order polynomial was used to describe the radial, and Delirhasannia *et al.* (2010) developed a model to simulate the application of water in a centre-pivot-irrigated field. Li *et al.* (1995) proposed an empirical model to fit the drop diameter distribution curve. Yan *et al.* (2010) modified the mathematical model of droplet ballistics and evaporation for sprinkler irrigation, and droplet size distribution models have been developed over several years (Solomon *et al.*, 1985). The aforementioned models indicated the water jet trajectory when the nozzles were full of water.

A new type of fluidic sprinkler (PXH) has been developed at Jiangsu University, China. The working theory for a fluidic sprinkler mainly depends on differential pressure control (Zhu *et al.*, 2009; Li *et al.*, 2011; Liu *et al.*, 2013). The nozzle of a fluidic sprinkler has two phases, gas and liquid. Limited work has been undertaken to compare the hydraulic parameters of PXH and other types of sprinkler. This study was designed to investigate the hydraulic performance of the newly developed PXH relative to other well-known and widely used sprinklers, and to establish a mathematical model of the PXH water distribution and droplet diameter. The main objectives of this research were to compare the hydraulic performance of individual PXHs and other types of sprinkler in indoor conditions and to introduce several empirical equations for use with the newly developed sprinkler.

MATERIALS AND METHODS

Four types of sprinkler heads were used in this study. The PXH was manufactured by Shanghai Watex Water-economizer Technology Co. Ltd., China, PY was manufactured by Shanghai Huawei Water Saving Irrigation Technology Co. Ltd., China, Toro S 800 was obtained from Toro Company, USA and RainBird S 3504 was obtained from RainBird Company, USA. The main differences between the PXH and the other sprinklers are their working principles. The working theory of the PXH primarily depends on the pressure difference between its left and right sides, which has not frequently been reported in the literature.

Working theory of the fluidic sprinkler

Fluidic sprinkler nozzles are filled with water and gas. A pressure differential can be created using a signal tube, and the water flow can be bent to provide the driving force. The cross section of the nozzle outlet is elliptical. An image of a fluidic sprinkler is shown in Figure 1.

The working process of the fluidic sprinkler is shown in Figure 2. Operation of the fluidic sprinkler includes stationary and rotating step-by-step modes that depend on the pressure differential between the left and right sides. First, air flows into the left side from Signal 3 while air enters the right side from Clearance C. The main flow jet is straight and the sprinkler remains stationary if the pressures are equal on both sides, as shown in Figure 2 (a). The signal water received from Signal 1 will fill up Signal 2 to induce a low-pressure eddy on the right side. Clearance C gradually decreases and eventually disappears. The main flow jet is bent towards and eventually attaches to the boundary because the left pressure is higher than the right pressure. Consequently, the sprinkler is driven to rotate, as shown in Figure 2 (b). When the main jet flow bends to the right, Signal 1 cannot receive any water. Next, the negative pressure between the left and right sides disappears as the water in the signal tube is sucked out. Thus, the main flow jet becomes straight, and the sprinkler becomes stationary. This process is repeated and self-controlled.

Experimental set-up and procedure

Performing experiments in an indoor facility ensures radial water distribution and avoids water drift and loss (Sourell *et al.*, 2003; Dukes, 2006). Any radial water distribution around the sprinkler can be represented by one radial under indoor laboratory conditions. In this work, an indoor experiment apparatus was set up in the experimental hall of the Research Centre of Fluid Machinery Engineering and Technology at Jiangsu University, China. The laboratory has a diameter of 44 m and a height of 18 m. No obstacles were

Figure 1. Image of a fluidic sprinkler.

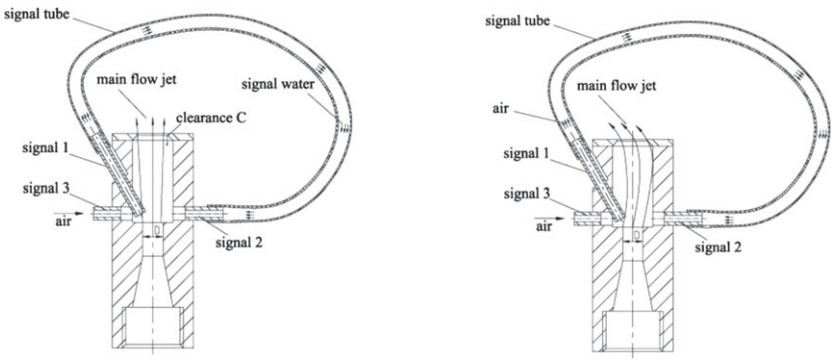

(a) Straight spray state (b) Stepping state

Figure 2. Geometrical elements of the fluidic sprinkler nozzle and its working process.

present in the laboratory, and wind interference was eliminated. A schematic of the sprinkler set-up is shown in Figure 3. The sprinkler was placed in the centre of the laboratory. The sprinkler heads were mounted on a 1.5 m riser at a 90° angle to the horizontal and were placed approximately 0.9 m above the top of the catch-cans.

The sprinkler system included a centrifugal pump (model IS80–50-250, manufactured by Foshan Pump Factory Co.

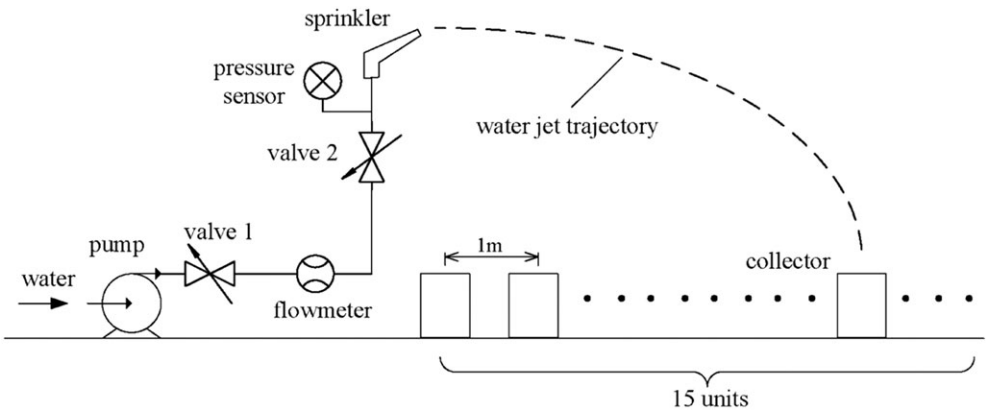

Figure 3. Experimental system.

Ltd., China), a pipeline, Valve 1, a flow meter (model E-mag E, manufactured by Kaifeng Instrument Co. Ltd., China), Valve 2, a pressure sensor (model MPM482, manufactured by Micro Sensor Co. Ltd., China), and sprinklers. The water was pumped through valve 1 before travelling through the flow meter, valve 2, and the sprinkler into the air. Valve 1 controlled the pump outlet pressure and the flow rate. The discharge was measured using a flow meter with an accuracy tolerance of 0.5%. The operating pressure of the sprinkler was measured using a pressure sensor with an accuracy tolerance of 0.4%. An operating pressure of 250 kPa was used to compare the PXH, PY, Toro S 800 and RainBird S 3504 sprinklers. The following four operating pressures were tested for the PXHs with nozzle diameters of 4, 6 and 8 mm: 200, 250, 300 and 350 kPa. All of these operating pressures are within the manufacturer's recommendations. The sprinkler was run for a few minutes to standardize the environmental conditions before performing the experiments. The experiment lasted for 1 h, and the flow rate and pressure from the nozzles used for the tests were measured three times under the same conditions. The collectors (manufactured by the Shanghai Meteorological Instrument Factory Co. Ltd., China) used in this study were 0.2 m in diameter and 0.6 m tall. Fifteen collector locations were distributed with 1 m spacing between the units along the radial. The point application rate was tested using a collector mould in an auto-testing system (Faci *et al.*, 2001; Hills and Barragan, 1998; Zhu *et al.*, 2009). The droplet diameter was measured at the observation point using the stain method (Zhu *et al.*, 2012). The experiments followed the standards of the American Society of Agricultural and Biological Engineers (2007: S398.1).

EXPERIMENTAL RESULTS AND ANALYSES

Although the operating conditions were controlled, they differed slightly between each measurement (in particular, operating pressures varied slightly), and the droplets measured on each occasion were different.

Water distribution

The working parameters and hydraulic parameters of the different types of sprinklers are shown in Table I. The water distributions of the sprinklers are shown in Figure 4.

Figure 4(a) presents the experimental observations from applying water using the different types of sprinkler. Comparing the water distributions from the four types of sprinkler heads under the same conditions showed that the PXH produced a lower average application rate than the PY and RainBird S 3504 sprinklers and a higher average application rate than the Toro S 800 sprinkler. These differences can be attributed to the flow rate factor. At the same operating pressure, the flow rates of the PY and RainBird S 3504 sprinklers were much higher and the flow rate of the Toro S 800 much lower than the PXH. The wetted radii were 12.5, 12.3, 11.8 and 11.5 m for the PXH, PY, RainBird S 3504 and Toro S 800 sprinklers, respectively. This comparison shows that the PXH produced the largest wetted radius under the test conditions, which may be attributed to the unique working principles of the PXH. When the PXH fulfilled its stationary and rotating step-by-step modes without any other interference, the main flow from the nozzle was thrown the furthest.

Table I. Working parameters and hydraulic parameters of the different types of sprinklers

Spray sprinkler type	Nozzle diameter (mm)	Operating pressure (kPa)	Flow rate ($m^3\ h^{-1}$)
PXH	4	250	1.26
PY	4	250	1.36
Toro S800	4	250	1.03
RainBird S3504	4	250	1.41

Figure 4(b) presents the radial application rate distribution profiles for the PXH with a nozzle diameter of 4 mm at 200, 250, 300 and 350 kPa. As the distance from the sprinkler increased, the water application rate increased to a maximum value before slowly decreasing. The application rates of PXH varied from 0 to 5.1 mm h^{-1} under different operating pressures. The maximum application rate was obtained for the four analysed pressures (2.6 mm h^{-1} at 4 m for 200 kPa, 3.2 mm h^{-1} at 4 m for 250 kPa, 4.2 mm h^{-1} at 5 m for 300 kPa, and 5.1 mm h^{-1} at 6 m for 350 kPa). Starting from this distance, the application rate decreased slowly until reaching a minimum. For 200 kPa at 11 m, 250 kPa at 12 m, 300 kPa at 13 m and 350 kPa at 13 m, the minimum values were 0.5, 0.6, 0.4 and 0.5 mm h^{-1}, respectively. The water distribution patterns from the PXH were similar under different operating pressures. Moreover, the water application rates were maintained at a distance between 0 and 6 m, and the range of the PXH working pressure was large enough to prevent the patterns from significantly changing. These advantages can be attributed to the mixing of air with water in the nozzle when the water is emitted from the PXH nozzle. The air in the nozzle destroys the structure of the water jet, improving the sprinkler performance.

Droplet size

Three metres from the sprinkler, the water droplets were small and travelled at a low-medium velocity. As the

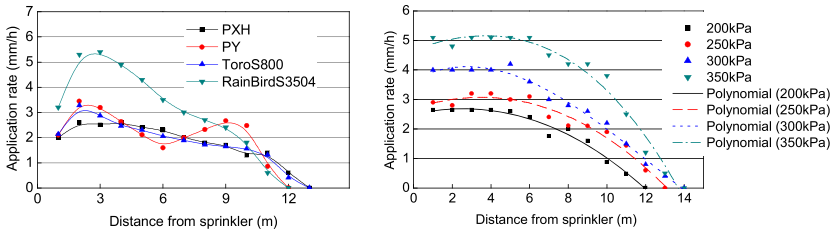

(a) Different types of sprinklers (b) PXHs at 200, 250, 300 and 350 kPa

Figure 4. Experimental water distribution.

distance increased from 3 m, the velocity gradually increased with distance. Finally, at the furthest point from the sprinkler, the velocities were medium-high and the largest drops appeared. The diameters of the experimental droplets are shown in Figure 5. Figure 5(a) presents the experimental observations for the droplet diameters from different types of sprinkler at an operating pressure of 250 kPa and measured at the position furthest from the sprinkler. Figure 5(b) presents the droplet diameter profiles versus their distance from the sprinkler for the PXH with a nozzle diameter of 4 mm at pressures of 200, 250, 300 and 350 kPa. The distances of the testing points from the sprinkler were 3, 5, 8 m, and at the end of the wetted radius.

As shown in Figure 5(a), PXH resulted in the smallest droplet diameters among all of the sprinkler types operating under the same conditions. The diameters of the droplets from the PXH were 20.3, 8.4 and 3.1% less than those from the PY, RainBird S 3504 and Toro S 800 sprinklers, respectively. The PXH had the smallest droplet diameter (Figure 5 (a)) and the longest wetted radius (Figure 4(a)). This finding does not completely agree with those obtained from ballistic models (Solomon *et al.*, 1985). These differences may be attributed to the dispersion of the water jet by the two-phase flow in the nozzle of the fluidic sprinkler, which transfers much less kinetic energy to the soil.

From Figure 5(b), it was observed that the data are similar at different operating pressures when the distance from the sprinkler is between 3 and 5 m. When the distance is greater than 5 m from the sprinkler, the droplet diameters were different at different operating pressures. The droplet diameter increased with distance, reaching a minimum of 0.25 mm at 3.0 m and a maximum of 3.45 mm at the end of the spray radius. For a given distance from the sprinkler, the droplet size generally decreased as the operating pressure increased. For example, when the distance from the sprinkler was 8 m, the droplet diameters were 2.81, 2.63, 2.38 and 2.20 mm at 200, 250, 300 and 350 kPa, respectively. The effects of pressure on droplet diameter were more evident for large distances from the sprinkler. Compared with an operating pressure of 200 kPa, the droplet diameter at the end of the wetted radius of the PXH decreased by 5.8, 10.1 and 15.9% at pressures of 250, 300 and 350 kPa, respectively.

ESTABLISHMENT OF A MATHEMATICAL MODEL FOR THE PXH

Water distribution model

Special attention was given to the development of empirical equations for the water distribution model regarding the distance that water travelled from the PXH sprinkler. In addition to the regression shown in Figure 4(b), a third-order polynomial regression line was fitted to the distance from the sprinkler and the application rate data to estimate the water distribution. The third-order polynomials used to describe the radial are shown in Table II, where y is the application rate and x is the distance from the sprinkler.

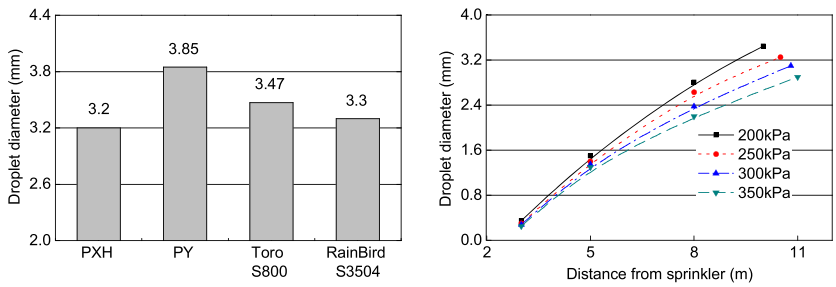

(a) Different types of sprinklers (b) PXH at 200, 250, 300 and 350 kPa

Figure 5. Experimental droplet diameter.

Table II. Regression analysis with third-order polynomials

Operating pressure (kPa)	Third-order polynomial	Coefficient of determination (%)
200	$y = 0.0016x^3 - 0.0665x^2 + 0.391x + 2.08$	96.8
250	$y = -0.0012x^3 + 0.0061x^2 - 0.0865x + 3.31$	95.1
310	$y = 0.0023x^3 - 0.018x^2 + 0.428x + 3.48$	98.8
350	$y = -0.0017x^3 - 0.0145x^2 + 0.164x + 4.82$	97.6

The coefficient of determination for PXH ranged from 95.1 to 98.8%, with an average of 97.1%.

Droplet size model

Droplet size, which depends on nozzle shape, nozzle diameter and operating pressure, is an important indicator of sprinkler irrigation performance and is important relative to wind resistance. Larger droplets are more resistant to wind drift. The fluidic sprinkler model used in this study is given by the following equation:

$$D = \xi d^a H^b \tag{1}$$

where D is the mean volume diameter of droplet size at the bottom of the wetted radius (mm); d is the nozzle diameter (mm); H is operating pressure head (m); and ξ, a and b are dimensionless parameters that can be obtained through regression analysis.

In this study, results were obtained using the stain method at the edge of the wetted radius. Figure 6 shows the droplet diameter at different operating pressures. The fluidic sprinkler nozzle diameters are 4, 6 and 8 mm, and the operating pressures are 200, 250, 300 and 350 kPa, respectively. As shown in Figure 6, the droplet diameter decreased as the operating pressure increased, with maximum values of 3.62, 4.35 and 4.87 mm for nozzle diameters of 4, 6 and 8 mm at 200 kPa, respectively. The minimum values were 2.71, 3.21 and 3.76 mm for the nozzle diameters of 4, 6 and 8 mm at 350 kPa, respectively. The droplet diameter for the PXH increased as the nozzle diameter increased. Compared with a nozzle diameter of 4 mm, the droplet diameters from nozzles with diameters of 6 and 8 mm increased by 20.2 and 34.5% at operating pressures of 200 kPa, 15.1 and 34.5% at 250 kPa, 21.2 and 36.3% at 300 kPa and 18.5 and 38.7% at 350 kPa, respectively.

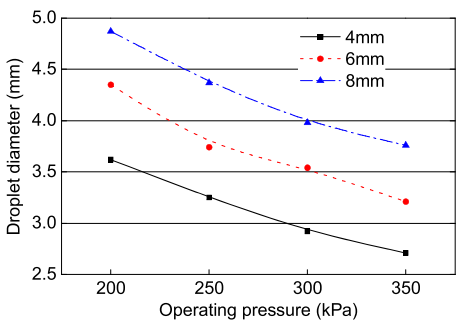

Figure 6. Droplet diameters at different operating pressure and from nozzles with different diameters.

Special attention was given to the development of empirical equations to model droplet size. Polynomial regressions were fitted to the operating pressure and to the distance from the sprinkler versus droplet size. The dimensionless parameters of ξ, a and b in Equation 1 are 14.4, 0.46 and −0.664, respectively. The droplet size model for PXH was proposed as shown in Equation 2.

$$D = 14.4\, d^{0.46} H^{-0.664} \tag{2}$$

Validation of the droplet size model

To verify the droplet size model for fluidic sprinklers, the predicted droplet diameters were compared with the measured values from the experiments. The fluidic sprinkler parameters for the different cases are shown in Table III.

Figure 7 shows a comparison between the predicted and measured droplet diameter data for the PXH. According to Figure 7, the predicted results are lower than the measured ones in four cases (cases 1, 3, 5 and 6) and larger than the

Table III. Fluidic sprinkler parameters for the different cases

Case number	Nozzle diameter(mm)	Operating pressure (kPa)
1	4	225
2	4	275
3	6	275
4	6	325
5	8	325
6	8	375

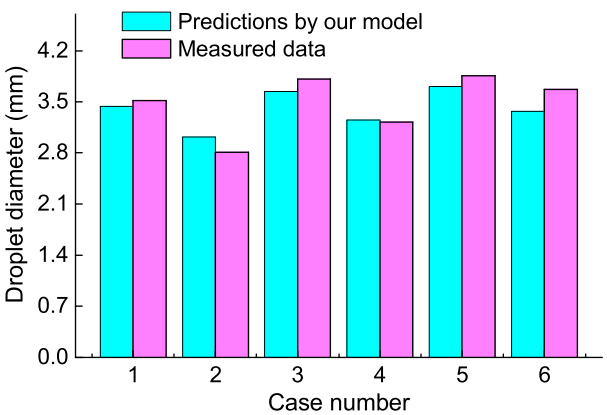

Figure 7. Comparison between the predicted and measured droplet diameter data for PXH.

measured results in two cases (cases 2 and 4). These differences can be attributed to the random experimental error for the measured data, which is inevitable and did not affect the accuracy of the droplet size model. For a given nozzle diameter, the droplets decreased as the operating pressure increased, which was proven by the predicted and measured results. This phenomenon partly confirmed the accuracy of the droplet size model. For a given increasing operating pressure (50 kPa in this study), the droplet size model indicated that the reduction value of the drop size decreased as the nozzle diameter increased. For example, the reduction value obtained from Equation 2 was 0.42 mm at the nozzle with a diameter of 4 mm, 0.39 mm at the nozzle with a diameter of 6 mm, and 0.34 mm at the nozzle with a diameter of 8 mm. The measured results present the same trends of the droplet size model, with a reduction value of 0.71 mm when the nozzle diameter is 4 mm, 0.59 mm when the nozzle diameter is 6 mm, and 0.19 mm when the nozzle diameter is 8 mm. This phenomenon again confirmed the accuracy of the droplet size model. The relative error between predicted and measured results varied from 0.9 to 8.9% in different cases. Case 6 had the highest relative error of 8.9%, and Case 3 had the lowest relative error of 0.9%. The average relative error was 4.6%. This comparison revealed that the predicted results fit the measured results well and that the established model accurately predicted the droplet size of the PXH.

CONCLUSIONS

1. A new fluidic sprinkler (PXH) prototype was presented. The working principle of the PXH consisted of two statistical conditions, the straight main flow jet and the main flow jet reattached to the right side. This process was repeated automatically to allow the PXH to rotate without external control;
2. When comparing the four different types of sprinkler, the PXH resulted in a lower average application rate than the PY and RainBird S 3504 sprinklers and a higher average application rate than the Toro S 800 sprinkler. The PXH produced the longest wetted radius, exhibited optimal water distribution performance, and resulted in the smallest droplet diameter. The water in the nozzle of the PXH was subjected to two-phase flow. The air in the nozzle destroyed the water jet fluid structure, improving the PXH's performance;
3. Empirical equations for the water distribution from the PXH were regressed, with coefficients of determination ranging from 95.1 to 98.8%. An empirical equation for the droplet size of the PXH ($D = 14.35\ d^{0.46}H^{-0.664}$) was reported in this study;
4. The droplet size model was verified based on the experimental results for six cases with different droplet diameters. The average relative error between the predicted and measured droplet diameters was 4.6%. The predictions from the model were in good agreement with the measured values.

ACKNOWLEDGEMENTS

The authors gratefully acknowledge the National Natural Science Foundation of China, No. 51309117, the China National High-Tech (863) Program Grant No. 2011AA100506, the Natural Science Foundation of the Colleges and Universities in Jiangsu Province, No. 13KJB210003, the Postdoctoral Science Foundation Special Support of China, No. 2014 T70484, the Senior Professionals Scientific Research Foundation at Jiangsu University, No. 13JDG028, and the 'Young Gugan Training Project' of Jiangsu University.

REFERENCES

American Society of Agricultural and Biological Engineers (ASABE). 2007. ASABE Standards (R2007). S398.1: Procedure for Sprinkler Testing and Performance Reporting. St Joseph, Mich., USA.

Al-Naeem MAH. 1993. Optimisation of Hosereel rain gun irrigation systems in wind; simulation of the effect of trajectory angle, sector angle, sector position and lane spacing on water distribution and crop yield. PhD dissertation, Silsoe College, Cranfield University, Cranfield, UK.

Branscheid VO, Hart WE. 1986. Predicting field distribution of sprinkler systems. *Transactions of the ASAE* **11**: 801–803.

Burt CM, Clemmens AJ, Strelkoff TS, Solomon KH, Bliesner RD. 1997. Irrigation performance measures: efficiency and uniformity. *Journal of Irrigation and Drainage Engineering* **123**(6): 423–442.

Carrion P, Tarjuelo JM, Montero J. 2001. SIRIAS: a simulation model for sprinkler irrigation: I. Description of the model. *Irrigation Science* **20**: 73–84.

Dechmi F, Playan E, Cavero J, Martinez-Cob A, Faci JM. 2004a. Coupled crop and solid-set sprinkler simulation model: I. Model development. *Journal of Irrigation and Drainage Engineering* **130**(6): 499–510.

Dechmi F, Playan E, Cavero J, Martinez-Cob A, Faci JM. 2004b. Coupled crop and solid-set sprinkler simulation model: II. Model application. *Journal of Irrigation and Drainage Engineering* **130**(6): 511–519.

Delirhasannia R, Sadraddini AA, Nazemi AH, Farsadizadeh D, Playan E. 2010. Dynamic model for water application using centre pivot irrigation. *Biosystems Engineering* **105**: 476–485.

Dukes MD. 2006. Effect of wind speed and pressure on linear move irrigation system uniformity. *Applied Engineering in Agriculture* **22**(4): 541–548.

Faci JM, Salvador R, Playan E, Sourell H. 2001. Comparison of fixed and rotating spray plate sprinklers. *Journal of Irrigation and Drainage Engineering* **127**(4): 224–233.

Fukui Y, Nakanishi K, Okamura S. 1980. Computer evaluation of sprinkler irrigation uniformity. *Irrigation Science* **2**: 23–32.

Hills D, Barragan JJ. 1998. Application uniformity for fixed and rotating spray plate sprinklers. *Applied Engineering in Agriculture* **14**(1): 33–36.

Li H, Yuan SQ, Xiang QJ, Wang C. 2011. Theoretical and experimental study on water offset flow in fluidic component of fluidic sprinklers. *Journal of Irrigation and Drainage Engineering* **137**(4): 234–243.

Li J, Li Y, Kawano H, Yoder RE. 1995. Effects of double-rectangular-slot design on impact sprinkler nozzle. *Transactions of the ASAE* **38**(5): 1435–1441.

Li J, Rao M. 2003. Field evaluation of crop yield as affected by nonuniformity of sprinkler-applied water and fertilizers. *Agricultural Water Management* **59**: 1–13.

Liu JP, Yuan SQ, Li H, Zhu XY. 2013. A theoretical and experimental study of a variable-rate complete fluidic sprinkler. *Applied Engineering in Agriculture* **29**(1): 17–24.

Montero J, Tarjuelo JM, Carrion P. 2001. SIRIAS: a simulation model for sprinkler irrigation: II. Calibration and validation of the model. *Irrigation Science* **20**: 85–98.

Playan E, Zapata N, Faci JM, Tolosa D, Lacueva JL, Pelegrin J, Salvador R, Sanchez I, Lafita A. 2006. Assessing sprinkler irrigation uniformity using a ballistic simulating model. *Agricultural Water Management* **84**: 89–100.

Richards PJ, Weatherhead EK. 1993. Prediction of rain gun application patterns in windy conditions. *Journal of Agriculture Engineering Research* **54**: 281–291.

Seginer I, Nir D, Bernuth RD. 1991. Simulation of wind-distorted sprinkler patterns. *Journal of Irrigation and Drainage Engineering* **117**(2): 285–306.

Smith RJ, Gillies M, Newell HG, Foley JP. 2008. A decision support model for traveling gun irrigation machines. *Biosystems Engineering* **100**: 126–136.

Solomon KH, Kincaid DC, Bezdek JC. 1985. Drop size distributions for irrigation spray nozzles. *Transactions of the ASAE* **28**(6): 1966–1974.

Sourell H, Faci JM, Playán E. 2003. Performance of rotating spray plate sprinklers in indoor experiments. *Journal of Irrigation and Drainage Engineering* **129**(5): 376–380.

Vories ED, Von Bernuth RD, Mickelson RH. 1987. Simulating sprinkler performance in wind. *Journal of Irrigation and Drainage Engineering* **113**(1): 119–130.

Yan H, Bai G, He JQ, Li YJ. 2010. Model of droplet dynamics and evaporation for sprinkler irrigation. *Biosystems Engineering* **106**: 440–447.

Zhu XY, Yuan SQ, Li H, Liu JP. 2009. Orthogonal tests and precipitation estimates for the outside signal fluidic sprinkler. *Irrigation and Drainage Systems* **23**(4): 163–172.

Zhu XY, Yuan SQ, Liu JP. 2012. Effect of sprinkler head geometrical parameters on hydraulic performance of fluidic sprinkler. *Journal of Irrigation and Drainage Engineering* **138**: 1019–1026.